Supporting Information

Ferrer *et al.* 10.1073/pnas.0800071105

SI Text

Strains, Proteins, and Standard Buffers. *F. acidiphilium* strain Y^T DSM12658 (*Fa*), was cultured at 37°C in 9K medium, pH 1.7, as described (1). *T. acidophilum* $DSM1728^T$ (*Ta*), *P. torridus* $DSM9790^T$ (*Pt*), *S. acidocaldarius* $DSM639^T$ (*Sa*), and *A. ferrooxidans* $DSM14882^T$ (*Af*) were obtained from the German Collection of Microorganisms and Cell Cultures (DSMZ, Braunschweig, Germany), and cultured as described (2). *E. coli* DH5α from Invitrogen used for site-directed mutagenesis, and *E. coli* BL21(DE3)pLysS and ORIGAMI(DE3)pLysS from Novagen used for gene expression, were cultured and maintained according to the recommendations of the suppliers. Unless otherwise stated, the standard buffers (100 mM) and conditions used in the present study were as follows: sodium citrate buffer, pH 3.0 and 40°C, for LigFa; sodium phosphate pH 6.5 and 70°C, for LigTa and LigPt; sodium phosphate pH 7.0 and 40°C, for LigAf; and sodium phosphate pH 7.5 and 80°C, for LigSa (pH was adjusted at 25°C in all cases).

Preparation of Ferric Nitroacetate [Fe(NTA)$_2$] Solution. $Fe(NTA)_2$ was freshly prepared by mixing 10 ml of ferric chloride ($FeCl_3$) (Sigma, 99%) solution (0.04 M) and 20 ml of nitroacetic acid (NTA) (Sigma, 99%) solution (0.08 M), as described (3, 4). Before use, the solution was filtered by centrifugation through a 0.45 μm Durapore membrane (Millipore) in an Eppendorf centrifuge (6,000 $\times g \times$ 5 min).

Preparation of Reduced and Metal Free LigFa Variants. $LigFa_R$ was prepared by mixing 3 ml of 0.27 mM stock solution of ferric-containing enzyme in 100 mM sodium citrate, pH 3.0, with 75 μl sodium dithionite stock solution (0.5 M in the same buffer) and incubation at 25°C for 3 h. The reduced enzyme was separated from excess reagent on a Sephadex G-25 column and lyophilized. To confirm that the protein was fully reduced, we recorded the time-course of absorbance change after mixing LigFa with dithionite. It is apparent from Fig. S7 that the reduction of LigFa was essentially complete after 3 h of incubation, as shown by the complete loss of absorption at 564 nm, typical of Fe(III)-Tyr interactions. We used Mössbauer spectroscopy to assess whether or not the reduction led to a mixed-valence state. ^{57}Fe-enriched LigFa was prepared as described below and 0.4 ml of a 1 mM stock solution was incubated for 3 h at 25°C with the dithionite (12.5 mM). The solution was then extensively dialyzed against sodium citrate pH 3.5 buffer through a Centricon YM-10 membrane, transferred into a Delrin cup (0.3 ml), and stored frozen until spectra were recorded. The 77K-spectrum of oxidized ^{57}Fe-enriched LigFa at pH3.5 showed a quadrupole doublet with isomer shift of 0.52 mm/s and quadrupole splitting of 0.65 mm/s, which are typical for high-spin iron(III). However, the 77K-spectrum of reduced protein showed a quadrupole doublet for high-spin iron(II). A further constraint for the fit was that the area ratio of both signals (Fe^{3+} versus Fe^{2+}) was 1:1, which is consistent with full reduction of the protein. Moreover, our measurements showed that the 77K-spectrum of reduced protein at pH 3.5 did not exhibit any doublet characteristic for Fe(II)/Fe(III) mixtures: localized mixed valency in a binuclear iron site would exhibit two different quadrupole doublets, one for Fe(II) and one for Fe(III). Therefore, we may conclude that the reduction was complete in our experiments.

$LigFa_{MF}$ was isolated by dissolving $LigFa_R$ (54 mg) in 100 mM sodium citrate, pH 3.0, supplemented with 10 mM EDTA, followed by 12 h incubation at 25°C, extensive dialysis against the same buffer through a Centricon YM-10 membrane, and lyophilization. Protein samples were stored at -20°C until use.

Preparation of LigFa Variants Containing Metals Other Than Iron. LigFa variants containing metals other than iron were prepared by equilibration of metal-free LigFa, prepared as described above, with a fresh solution of metal nitrilotriacetate. To prepare the metal nitrilotriacetate [M^{n+}(NTA)], one ml of a metal chloride solution (Sigma; >99%) (40 mM in water) was mixed with 2 ml of 80 mM NTA solution (in water), which was then adjusted to pH 3.5. 100 μl of a 0.31 mM stock solution of metal-free protein in 100 mM sodium citrate buffer, pH 3.5, and 10 μl of M^{n+}(NTA) solution were mixed at 25°C for 1 h, then extensively dialyzed against the same buffer through a Centricon YM-10 membrane, lyophilized and stored at -20°C until use. The following metals were tested: Na, Mg, Ca, Sr, Ti, V, Cr, Mn, Fe, Co, Ni, Zn, Ga, Al, Ru, W, and Re, but only those enzyme variants showing ligation activity are shown.

Other DNA Ligase Assays (Not Standard). Two other assays were used to characterize ligation capability. First, ligation of cohesive-ended DNA fragments: *Sau*3A-digested bacteriophage λ DNA fragments were prepared by incubating 2 μg λ DNA with 10 U of restriction enzyme for 60 min at 37°C, after which the reaction was stopped by addition of EDTA to 50 mM and heating, according to the protocol of the manufacturer (New England Biolabs), and the reaction mixture dialyzed twice in Microcon-100 columns (Amicon). The ligation reaction mixture contained 1 μg of *Sau*3a λ DNA fragments and 20 nM ligase in 100 mM buffer, 0.1 mM ATP, 10 mM DTT, and was incubated at 40°C (for LigFa and LigAf), 70°C (for LigTa and LigPt) or 80°C (for LigSa) for 120 min. Second, ligation of blunt-ended DNA fragments: SspI-digested ϕX174 DNA fragments were prepared by incubating 2 μg DNA with 10 units of restriction enzyme for 60 min at 37°C, after which the reaction was stopped and the mixture dialyzed as above. The reaction mixture contained 1 μg SspI fragments of bacteriophage ϕX174 DNA and 20 nM ligase in 100 mM buffer, 0.1 mM ATP, 10 mM DTT, and was incubated at 40°C (for LigFa and LigAf), 70°C (for LigTa and LigPt) or 80°C (for LigSa) for 12 h. Both reactions were terminated by addition of 5-μl stop/loading buffer [98% (vol/vol) formamide, 10 mM EDTA, 0.05% bromophenol blue, 0.05% xylene cyanol, and 0.2% SDS] followed by heating at 95°C for 5 min (for LigFa, LigTa and LigFa) or 110°C for 10 min (for LigPt and LigSa). DNA ligation products were analyzed by electrophoresis on a 10% polyacrylamide gel containing 7 M urea (nick-joining assay) or a 0.75% agarose gel (cohesive and blunt end ligations). Gels were stained with ethidium bromide and DNA bands were quantified, when necessary, by densitometric analysis (Gel-Pro Analyzer 4.0, MediaCybernetics).

EMSA. The double-stranded DNA used for ligase binding assays was obtained by annealing a 5′-^{32}P-labeled 35-mer oligonucleotide (5′-TAA GCT CCG GAT TGT CCG GGA GGT AAA GCC CTG AT-3′) with its nonphosphorylated complementary strand, followed by purification on 10% polyacrylamide gels. This double-stranded DNA is not a substrate for the ligation activity of LigFa but binds to the enzyme to form a protein-DNA complex. Briefly, the 5′-phosphorylated 35-mer single stranded oligonucleotide (5 μg) was dephosphorylated and then labeled with [[γ]-^{32}P]-ATP (50 μCi, 4500 Ci/mmol; ICN, in 2 μM unlabeled ATP), using T4 polynucleotide kinase (Roche Mo-

lecular Biochemicals). Unincorporated nucleotides were removed using Nuc-Trap columns (Stratagene) and the labeled oligonucleotide was then mixed with an equimolar amount of the non-phosphorylated corresponding complementary sequence, incubated at 85°C for 10 min, then slowly cooled to room temperature to allow annealing and purified on a 10% polyacrylamide gel. Protein–DNA complexes were allowed to form by incubation of the enzyme (0.5 μg) with labeled double stranded oligonucleotide at different concentrations in binding buffer (100 mM sodium citrate, pH 3.0, 1 mM DTT, 0.1 mg/ml BSA) on ice for 20 min, then at room temperature for 15 min. Complex formation was stopped by addition of 2 ml of stop buffer (30% glycerol and 0.25% bromophenol blue in 1× TBE). Control EMSA reactions were done under identical conditions with denatured protein obtained by incubating the enzyme (0.5 μg) in 100 mM sodium citrate buffer, pH 3.5 at 90°C for 5 min (lost of secondary structure was confirmed by CD analysis). Samples were analyzed by electrophoresis on an 8% non-denaturing polyacrylamide gel at 15 mA in prechilled 1×TBE, after which gels were fixed, dried and subjected to autoradiography. The autoradiogram was subsequently scanned with a Molecular Dynamics densitometer and approximate quantities of protein-DNA complexes were derived by volume integration of band intensities, using ImageQuant software. It should be noted that two ^{32}P- labeled bands can be observed in EMSA polyacrylamide gels: one less mobile band, corresponding to the DNA- enzyme complex, and a faster migrating band corresponding to uncomplexed DNA.

Cloning, Hyperexpression, and Purification of DNA Ligases. The gene for the ATP-dependent DNA ligase LigFa (595 aa, MW 67,841 Da; pI, 5.13), was PCR-amplified from genomic DNA isolated from *F. acidiphilum* cells using oligonucleotide primers LigFaFNde (5′-ACA TAT GAC AAA ATC TTA TAA TAT AC) and LigFaRBam (5′-TGG ATC CTT ATT TTG TTT TTT TCT GCA TTT) (endonuclease sites for NdeI and BamHI are shown in bold). Amplification conditions were as follows: 95°C–120 s, 30×[95°C–45 s, 50°C–60 s, 72°C–120 s], 72°C–500 s. The ≈1,800 bp *ligFa* PCR product was purified by agarose gel electrophoresis, extracted by means of a QiaExII Gel Extraction Kit (Qiagen), cloned into the pCR2.1 plasmid by means of the TOPO TA Cloning kit (Invitrogen), as recommended by the supplier, and introduced into *E. coli* DH5α electrocompetent cells (Invitrogen) by electroporation. Positive clones were selected on LB agar supplemented with kanamycin (50 μg/ml) and X-gal (5 mg/ml). Plasmid pCRLig harboring the PCR-amplified DNA fragment was isolated using Plasmid Mini Kit (Qiagen) and sequenced using M13 and rM13 oligonucleotide primers. The fragment containing the coding sequence for LigFa was excised from this plasmid by endonucleases NdeI and BamHI, gel-purified as above and ligated (14°C, 16 h, T4 DNA ligase from New England Biolabs) into the pET-3a plasmid vector (Novagen) that had been predigested with same endonucleases and dephosphorylated with shrimp alkaline phosphatase (Roche) at 37°C for 1 h. Ligation mixtures were transformed into *E. coli* DH5α electrocompetent cells (Invitrogen) that were subsequently plated on LB agar supplemented with 50 μg/ml ampicillin. Plasmid pET-3aLig was subsequently isolated and introduced into the *E. coli* BL21(DE3)pLysS expression host by heat-shock transformation, according to the suppliers' protocols (Novagen). The transformation mixtures were plated on LB agar supplemented with chloramphenicol (34 μg/ml) and ampicillin (50 μg/ml). The gene sequence coding for the LigFa ATP-dependent DNA ligase and its polypeptide translation sequence have been submitted to the EMBL/DDBJ/GenBank databases under accession number AJ850915.

The genes for ATP-dependent DNA ligases LigTa [588 aa; MW 66537.92 Da; pI 5.15], LigPt [590 aa; MW 66969.12 Da; pI 5.80], LigSa [598 aa; MW 67575.83 Da; pI 5.72] and LigAf [671 aa; MW 73885.09 Da; pI 6.37], from *T. acidophilum, P. torridus, S. acidocaldarius* and *A. ferrooxidans*, respectively, were PCR-amplified from *T. acidophilum, P. torridus, S. acidocaldarius* and *A. ferrooxidans* genomic DNA in a similar fashion with the following oligonucleotide primers: LigTaPstF (5′- ACT GCA GTT TTC CGT AGT TGC AGA TGC) and LigTaXhoR (5′-TCT CGA GTT AAC TCT TCT CCT CCG TTA TAG), LigPtPstF (5′- ACT GCA GTA TAT AAA TAT GGA TTT CTC G) and LigPtSalR (5′-TGT CGA CTT AAC TCT TCT CAA TAA CCT TTT), LigAfNdeF (5′-ACA TAT GGA GCG GGT CAA CCA TAC TGA C) and LigAfXhoR (5′-TCT CGA GTT CCT TTT CTG AAA ACA TCG CCA AA), LigSaPstF (5′-ACT GCA GTT TAA ATT AAT TGC TGA ATA TTT TGA C) and LigSaXhoR (5′-TCT CGA GTG TCT CTG TTA TGT CCT CAA CTT TC) (endonuclease sites for PstI, NsiI, NdeI and XhoI are shown in bold). Cloned PCR products were excised with PstI and XhoI (LigTa and LigSa), PstI and SalI (LigPt), and NdeI and XhoI (LigAf), gel-purified and ligated into the pET-31b(+) plasmid vector (Novagen) that had been predigested with endonucleases NsiI and XhoI (for LigTa, LigPt and LigSa), or with NdeI and XhoI (for LigAf), and dephosphorylated. Plasmids were subsequently isolated and introduced into *E. coli* ORIGAMI(DE3)pLysS expression host.

Heterologous Expression and Purification of Ligases. For enzyme expression and purification, overnight cultures of *E. coli* BL21(DE3)pLysS harboring the *ligFa* gene, or *E. coli* ORIGAMI(DE3)pLysS containing other ligase genes, were diluted 1:10 in Luria-Bertani (LB) liquid medium with appropriate antibiotics and grown at 37°C until the absorbance at 600 nm reached 0.6. Hyperexpression was then induced by addition of isopropyl-β-D-galactopyranoside (IPTG) to 0.5 mM, and incubation continued for a further 12 h.

Purification of LigFa. Cells were harvested, resuspended in LigFa standard buffer containing one protease inhibitor mixture tablet and DNase I grade II, incubated on ice for 30–45 min, and then sonicated for a total of 4 min. The soluble fraction was separated from debris by centrifugation (10,000 ×*g*, 30 min, 4°C), dialyzed overnight against the same buffer, and concentrated by ultrafiltration on a Centricon YM-10 membrane (Amicon, Millipore) to a volume of 1 ml. The concentrated protein solution (100 mg/ml) was incubated with 0.01 M freshly prepared $Fe(NTA)_2$ solution for a period of 1 h at room temperature followed by extensive dialysis against standard buffer in Centricon filter centrifuge cones (MW cutoff: 10 kDa; Millipore), to remove unbound iron, and further concentrated to a final volume of 1 ml. The extract was applied to a HiPrep 16/10 SP XL column (Amersham Pharmacia Biotech) equilibrated with LigFa standard buffer and eluted with a 0 to 1 M NaCl linear gradient. Enzyme peak fractions eluting at approx. 0.15 M NaCl were collected, concentrated on a Centricon YM-10 membrane to a final volume of 1 ml, and applied to a Superose 12 HR 10/30 gel filtration column preequilibrated with LigFa standard buffer containing 150 mM NaCl. Separation was performed at 4°C at a flow rate of 0.5 ml/min. The thus purified dark purple enzyme was dialyzed against LigFa standard buffer and stored at –20°C as lyophilized powder. N-terminal sequencing verified its authenticity.

Purification of LigTa, LigAf, LigSa, and LigPt. Cells were harvested by centrifugation, resuspended in lysis buffer (50 mM phosphate buffer pH 7.5, 10 mM 2-mercaptoethanol, 1 mM EDTA, 0.1 μg/ml lysozyme) and disrupted by sonication. $(NH_4)_2SO_4$ was then added to the supernatant fluid to 40% (wt/vol) and salted out proteins were removed by centrifugation (10,000 × *g* for 10 min). The supernatant fluid was diluted two-fold in Tris–HCl buffer (50 mM Tris·HCl, pH 7.5, DTT 1 mM, EDTA 1 mM),

loaded on a Resource Q (Amersham Pharmacia Biotech) column that was previously equilibrated with the same buffer and eluted with a linear gradient of NaCl (0–1 M in Tris·HCl buffer, pH 7.5). Active fractions eluting around 0.18–0.28 M NaCl were combined, concentrated to 1 ml (Centricon 10 kDa, Millipore), and loaded onto a Superdex-200 column (50 cm × 16 mm diameter, Amersham Pharmacia) that was equilibrated and developed with Tris–HCl buffer (50 mM Tris·HCl, pH 6.5, DTT 1 mM, EDTA 1 mM). Purified enzymes were then dialysed against Tris·HCl buffer (50 mM Tris·HCl, pH 6.5, DTT 1 mM, EDTA 1 mM) and stored at -20°C at a concentration of 50 μM.

SDS/PAGE was performed on 12% (vol/vol) acrylamide gels according to Laemmli (5). Purity was ascertained by silver staining and, in all cases, the enzymes were judged to be more than 95% pure. Protein concentrations were determined according to Bradford (6), with BSA as standard.

Site-Directed Mutagenesis. To identify potential tyrosine residues acting as iron ligands, single mutations were introduced into the *ligFa* gene that replaced Tyr residues at positions 5, 9, 11, 12, 55, 65, 97, 127, 129, 151, 159, 165, 204, 262, 264, 303, 338, 369, 426, 442, 468, 476, 528 and 588, with Thr. To assess the significance of residues in LigFa differing from highly conserved residues in other DNA ligases, or from those in the Fac ligase of *F. acidarmanus*, single mutations designed to produce the substitutions Glu^{132}Lys, Asp^{162}Glu, Asn^{255}→Gly, Thr^{491}→Ser, Ala^{575}→Pro, Phe^{192}→Ser, Phe^{363}→Thr and Pro^{559}→Lys were introduced into *LigFa*. Mutations were introduced into the plasmid pET-3aLig using the QuikChange procedure (Stratagene) with oligonucleotide pairs synthesized by Sigma-Genosys. Mutations were confirmed by DNA sequencing using the sequencing primers CH325 (5′-ATT CGT GAA AAA ATG GAA CAG A-3′), CH711 (5′-AGT GAT GCT GGC GGA ACG TCT GCG TAG CA-3′), and CH1618 (5′-ATT ACC GTG AGC CCG ATT CAT AC-3′). Primers were designed using software Primer Express using the *ligFa* gene sequence. The resulting variant plasmids were first transferred into *E. coli* DH5α and selected on the LB agar supplemented with ampicillin (50 μg/ml), and then into *E. coli* BL21(DE3)pLysS cells that were plated on LB agar supplemented with chloramphenicol (34 μg/ml), and ampicillin (50 μg/ml). Mutant proteins were produced and purified using the same protocol as for the wild-type protein.

Enzyme Characterization.

pH and Temperature Optima. The pH and temperature optima in the range of pH 1.0–8.0 and 15–100°C were determined. The buffers (100 mM) used were: sodium citrate (pH 1.0–3.0), sodium acetate (pH 3.0–5.0), Mes (pH 5.0–7.0) and Hepes (pH 7.0–8.0). The stability of the LigFa enzyme values was assessed by preincubating the enzyme in buffers with pH values ranging from 2.0 to 5.0 at 40°C, and measuring the residual activity using the standard assay. pH was always adjusted at 25°C.

Metal content. The metal ion content was measured with a high-resolution Perkin–Elmer Life Sciences HR-ICP-MS (model PE ELAN 6100 DRC), after dilution of 50 μg of the enzyme with 5 ml of 0.5% (vol/vol) HNO_3 to digest the protein and release metal ions (this solution was used without any further manipulation.

Circular Dichroism Spectroscopy and Analysis. Circular dichroism spectra (CD) were acquired between 190 and 255 nm with a Jasco J-720 spectropolarimeter equipped with a Peltier temperature controller, employing a 0.1 mm cell at 25°C. The LigFa concentration was determined spectrophotometrically (ε_{280} = 52322 M^{-1} cm^{-1}, calculated from the amino acid sequence at www.expasy.org/tools/protparam.html).

Spectra were analyzed with CD software from UMDNJ (www2.umdnj.edu/cdrwjweb) (7) and at DICHROWEB (http://public-1.cryst.bbk.ac.uk/cdweb) (8). The variable selection method CDSSTR (9) gave the best fitted model spectra. The other programs used were CONTIN (10), SELCON3 (11), K2D (12), as well as least squares fitting by linear combinations of the T&J33, S&W17, Fasman and Yang data sets (7). The results from the eight procedures were averaged.

UV-Visible Absorption Spectra. Absorption spectra of pure protein solution (0.3 mM in 100 mM buffer with appropriate pH) were measured in an optical cell, 1 cm-path, at 25°C in a UVIKON 930 spectrophotometer (Kontron Instruments) equipped with a temperature control unit. The loss or gain of iron by LigFa was monitored by changes in absorption at 564-nm, the characteristic ligand-to-metal charge-transfer band of iron-LigFa.

Mössbauer Experiments. ^{57}Fe-enriched LigFa was prepared for Mössbauer spectroscopy by a slight modification of the protocol described by Kretchmar *et al.* (3). Briefly, a ^{57}Fe-enriched ferric chloride solution was prepared by heating the metal (36 mg) in 5 M HCl (5 ml) containing few drops of concentrated HNO_3. The final concentration of $^{57}FeCl_3$ was 7 mM. Equal volumes of the $^{57}FeCl_3$ solution and 14 mM NTA in water were then mixed and the pH was adjusted to either 3.5 or 5.5. A mixture of 0.4 ml of a 1 mM stock solution of $LigFa_{MF}$, prepared as described above, and 0.12 ml $^{57}Fe(NTA)_2$ was then incubated for 1 h at 25°C, and then extensively dialyzed against the same buffer through a Centricon YM-10 membrane, and transferred into a Delrin cup (0.3 ml) and stored in frozen state until the spectra were recorded.

To test the possibility of direct binding of ^{57}Fe metal to DNA substrate, a mixture of 0.4 ml of a 1 mM stock solution of *Sau*3A-digested bacteriophage λ DNA fragments prepared as above (in 100 mM sodium citrate buffer, pH 3.5) was incubated for 1 h at 25°C with 0.12 ml $^{57}Fe(NTA)_2$, and then processed as for the LigFa sample.^{57}Fe-DNA-enriched LigFa was prepared by mixing 0.2 ml of a 2 mM stock solution of *Sau*3A-digested bacteriophage λ DNA fragments prepared as above (in 100 mM sodium citrate buffer, pH 3.5) with 0.2 ml of 2 mM stock solution of ^{57}Fe-enriched LigFa for 1 h at 25°C, and processed for Mössbauer spectroscopy as above .

Mössbauer spectra of ^{57}Fe-enriched LigFa, 1 mM, were recorded using a spectrometer in the constant acceleration mode. Isomer shifts are given relative to α-Fe at room temperature. The spectra obtained at 77, 140 and 190K were measured in a continuous flow cryostat (Oxford). Spectra were analyzed by least-squares fits using Lorentzian line shape. The temperature variation of measured six-line spectra (sextet) was analyzed for superparamagnetic behavior of iron-containing clusters (13).

Spectroelectrochemistry. The electrochemical mediator, methyl viologen (MV^{2+}) dichloride hydrate (Sigma-Aldrich, 98%), was dissolved in a 100 mM citrate buffer solution, pH 3.5, 2M KCl to a concentration of 0.5 mM. Sodium citrate was selected as the buffer because LigFa is fully active at this pH. For each experiment, a solution of 0.88 mM enzyme was used, using an electrochemical cell previously described (14).

1. Golyshina OV, *et al.* (2000) *Ferroplasma acidiphilum* gen nov, sp nov, an acidophilic, autotrophic, ferrous-iron-oxidizing, cell-wall-lacking, mesophilic member of the *Ferroplasmaceae* fam nov, comprising a distinct lineage of the *Archaea. Int J Syst Evol Microbiol* 3:997–1006.

2. Ferrer M, Golyshina OV, Beloqui A, Golyshin PN, Timmis KN (2007) The cellular machinery of *Ferroplasma acidiphilum* is iron-protein dominated. *Nature* 445:91–94.

3. Kretchmar AA, Teixeira M, Huynh BO, Raymond KN (1998) Mössbauer studies of electropjoretically purified monoferric and diferric human transferring. *Biol Metals* 1:26–32.
4. Jeon SJ, Ishikawa K (2003) Characterization of novel hexadecameric thioredoxin peroxidase from *Aeropyrum pernix* K1. *J Biol Chem* 278:24174–24180.
5. Laemmli UK (1970) Cleavage of structural proteins during the assembly of the head of bacteriophage T4. *Nature* 227:680–685.
6. Bradford MM (1976) A rapid and sensitive method for the quantification of microgram quantities of protein utilizing the principle of protein-dye binding. *Anal Biochem* 72:248–254.
7. Greenfield NJ (2006) Using circular dichroism spectra to estimate protein secondary structure. *Nature Protocols* 1:2876–2890.
8. Whitmore L, Wallace BA (2004) DICHROWEB, an online server for protein secondary structure analyses from circular dichroism spectroscopic data. *Nucl Acid Res* 32:W668–773.
9. Manalavan P, Johnson WC (1987) Variable selection method improves the prediction of protein secondary structure from circular dichroism spectra. *Anal Biochem* 167:76–85.
10. Provencher SW, Glöckner J (1981) Estimation of globular protein secondary structure from circular dichroism. *Biochemistry* 20:33–37.
11. Sreerama N, Woody RW (1994) Poly(pro)II helices in globular proteins: identification and circular dichroic analysis. *Biochemistry* 33:10022–10025.
12. Andrade MA, Chacón P, Merelo JJ, Morán F (1993) Evaluation of secondary structure of proteins from UV circular dichroism spectra using an unsupervised learning neural network. *Protein Eng* 6:383–390.
13. Trautwein AX, Bill E, Bominaar EL, Winkler H (1991) Iron containing proteins and related analogs – Complementary Mössbauer, EPR and magnetic susceptibility studies. *Struct Bonding* 78:1–91.
14. Moss D, Nabedryk E, Breton J, Mäntele W (1990) Redox-linked conformational changes in proteins detected by a combination of infrared spectroscopy and protein electrochemistry. Evaluation of the technique with cytochrome c. *Eur J Biochem* 187:565–572.

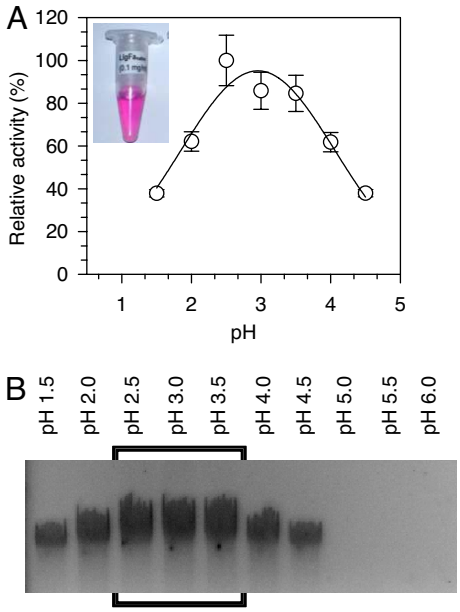

Fig. S1. Native LigFa has features similar to those of the recombinant. (*A*) Relative nick-joining ligation of native protein as calculated by gel densitometry. Assay conditions and buffers as in Fig. 1. *Inset* shows the color of native (0.1 mg/ml) preparation at pH 3.0. A typical scanned gel the pH-dependence of reaction by native LigFa at each of different pHs is shown in *B*.

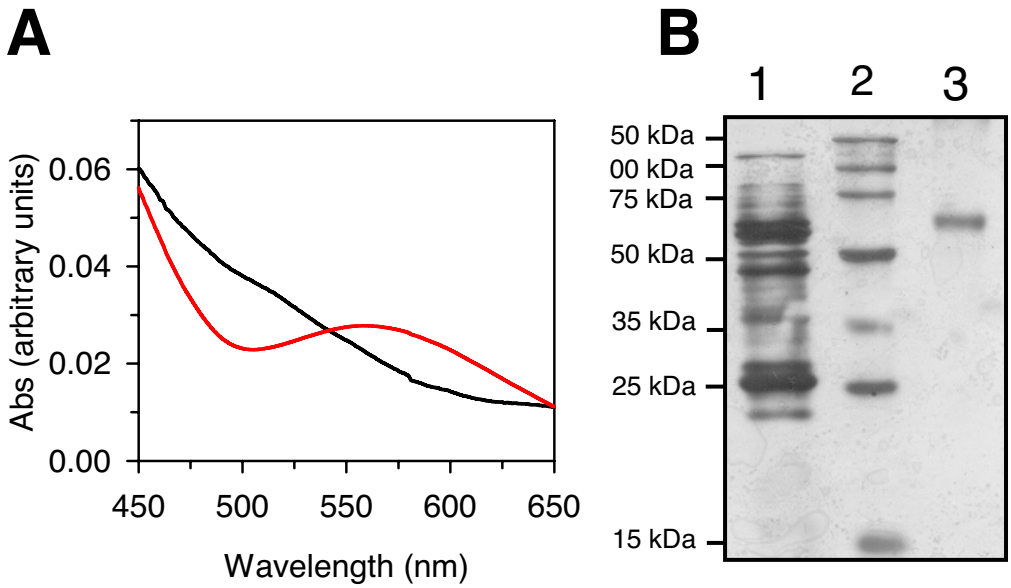

Fig. S2. Preparation of functional recombinant DNA ligase from *F. acidiphilum* (LigFa) in *E. coli* requires iron and low pH. (*A*) UV-Vis absorbance spectrum of *E. coli* cell extract suspension obtained before (black line) and after iron (red line) incorporation shows the characteristic λ_{max} at 564 nm in extracts supplemented with iron. Here we observed that iron is tightly bound through tyrosine residues (which gives the purple color; see main text) in the protein after incubation with freshly prepared $Fe(NTA)_2$. (*B*) SDS/PAGE of the purified LigFa. Samples were loaded as follows: *lane 1*, crude extract of induced *E. coli* BL21(DE3)pLysS harbouring pET-3aLigFa; *lane 2,* molecular mass markers (15–150 kDa, Novagen); *lane 3,* purified LigFa.

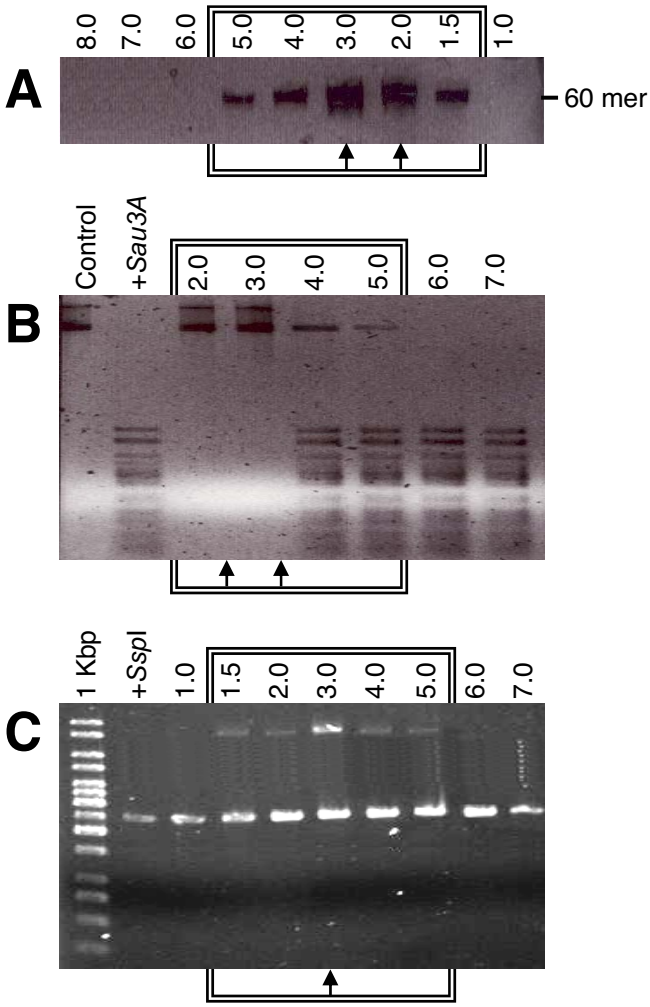

Fig. S3. Uniquely low pH activity optimum of LigFa with different substrates. (*A*) Nick-joining reaction with a substrate of two short oligonucleotides (25- and 35-mers) annealed to a 70-mer complementary oligonucleotide (only the region corresponding to the ligation product is shown); (*B*) ligation of *Sau*3a-generated sticky-ended fragments of bacteriophage λ DNA (*lane* 1, no enzyme added; *lane* 2, *Sau*3a-digested λ DNA; *lanes* 3–8, ligation activity at different pHs); c, ligation of SspI-generated blunt-ended fragments of ϕX174 DNA (*lane* 1, 1 kbp DNA ladder marker; *lane* 2, no enzyme added; *lanes* 3–8, ligation activity at different pHs).

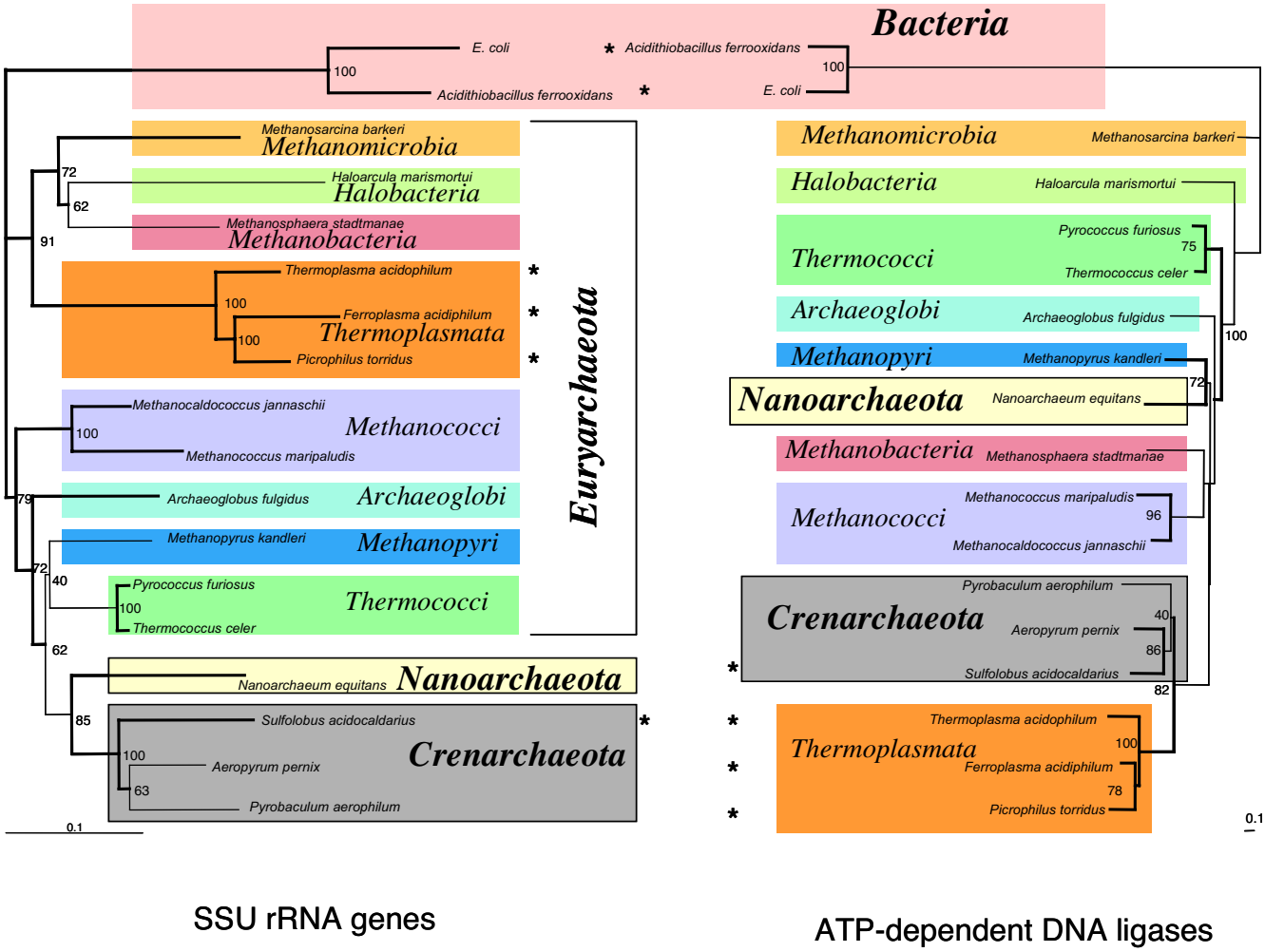

Fig. S4. Phylogeny of archaeal DNA ligases. Shown is a comparison of phylogenetic trees based on 16S rRNA gene sequences and amino acid sequences of the ATP-dependent DNA ligases of the principal archaeal taxa with fully sequenced genomes. Alignments were made with the ClustalW online tool (http://www.ebi.ac.uk) and analyzed with the DNADIST and PROTDIST PHYLIP packages (for calculation of distance matrix. The NEIGHBOR program (PHYLIP) was used to construct phylogenetic trees, by means of the Neighbor-joining method of Dayhoff PAM matrixmodel. Bootstrap values were calculated using SEQBOOT from the PHYLIP package. The tree was visualized using TreeView software. Robust clusters are shown with bold lines. Asterisks mark the organisms producing the ligases characterized in this work. Sequence accession numbers used for the construction of phylogenetic trees: *Picrophilus. torridus* DSM 9790, NC_005877; *Thermoplasma acidophilum* DSM 1728, NC_002578; *Ferroplasma acidiphilum* DSM 12658, ligase - AJ850915, 16SrRNA gene - AJ224936; *Sulfolobus acidocaldarius* DSM 639, NC_007181; *Aeropyrum pernix* K1, NC_000854; *Haloarcula marismortui* ATCC 43049, NC_006396; *Methanosarcina barkeri* str. *fusaro*, NC_007355; *Methanopyrus kandleri* AV19, NC_003551; *Methanococcus maripaludis* S2, NC_005791; *Nanoarchaeum equitans* Kin4-M, NC_005213; *Pyrococcus furiosus* DSM 3638, NC_003413; *Thermococcus kodakarensis* KOD1, NC_006624; *Archaeoglobus fulgidus* DSM 4304, NC_000917; *Escherichia coli* K12, NC_000913; the *Acidithiobacillus ferrooxidans* ATCC 23270, ligase was retrieved after BLASTing the *E. coli* DNA ligase against the *A. ferrooxidans* genome at the TIGR web site (www.tigr.org), 16S rRNA gene - AJ278718; *Pyrobaculum aerophilum* IM2, NC_003364; *Methanosphaera stadtmanae* DSM 3091, NC_007681; *Methanocaldococcus jannaschii* DSM 2661, NC_001732. As shown here, the rRNA gene sequence-based phylogenetic tree of the representatives of the principal archaeal genera with fully sequenced genomes generally exhibited higher robustness than the amino acid sequence-based phylogenetic tree of deduced ATP-dependent DNA ligases from the same organisms. The major difference was exhibited by the phylum *Euryarchaeota*, almost all classes of which clustered together. The deep-branching phyla *Nanoarchaeota* and *Crenarchaeota* clustered by rRNA and DNA ligase sequences with classes *Methanopyri* and *Thermococci* of the *Euryarchaeota*, but with a rather uncertain tree topology, although robust tree topology with bootstrap values of 70–100% was observed in both types of tree at the level of the classes (e.g., within *Thermoplasmata*, *Thermococci* and *Methanococci*) and within the phylum *Crenarchaeota*.

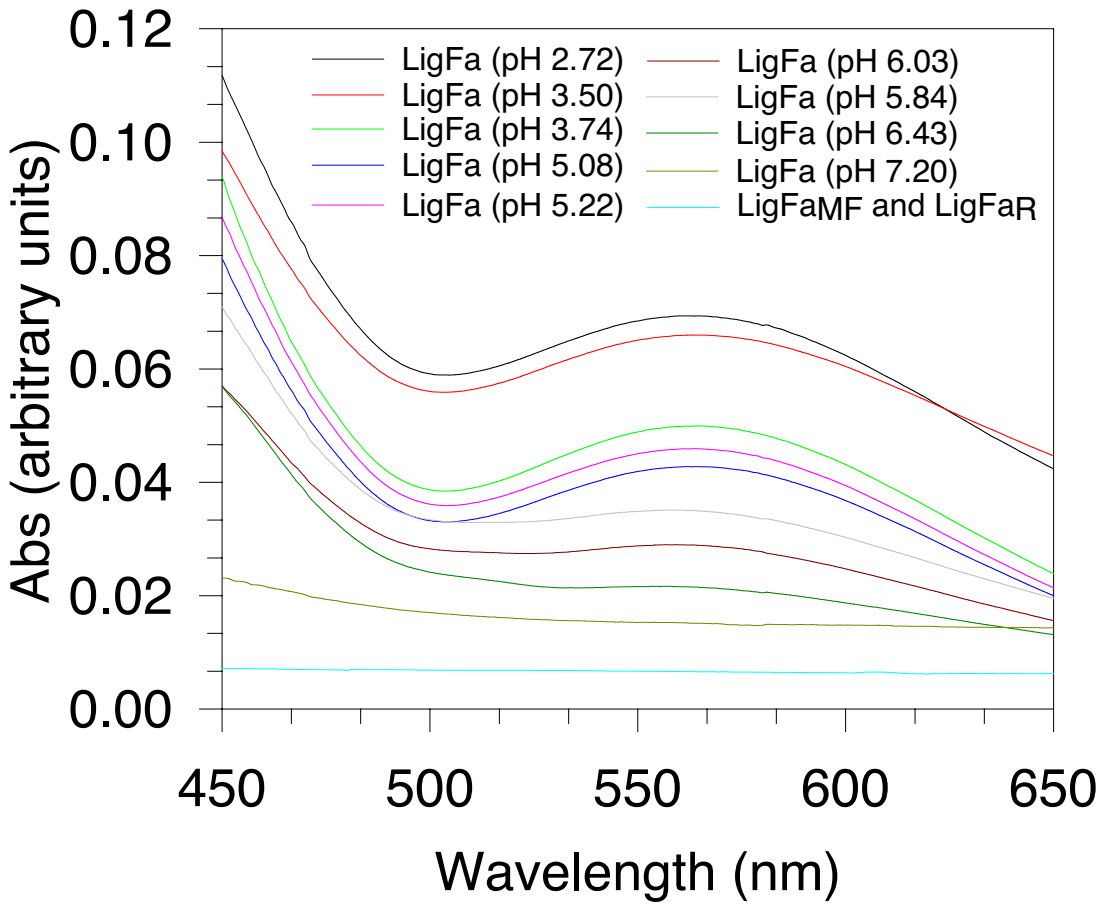

Fig. S5. UV-Vis absorption spectra produced by changing pHs in the LigFa preparation. The characteristic absorption has λ_{max} at 564 nm. [E] = 0.3 mM. Buffers were as in Fig. 1.

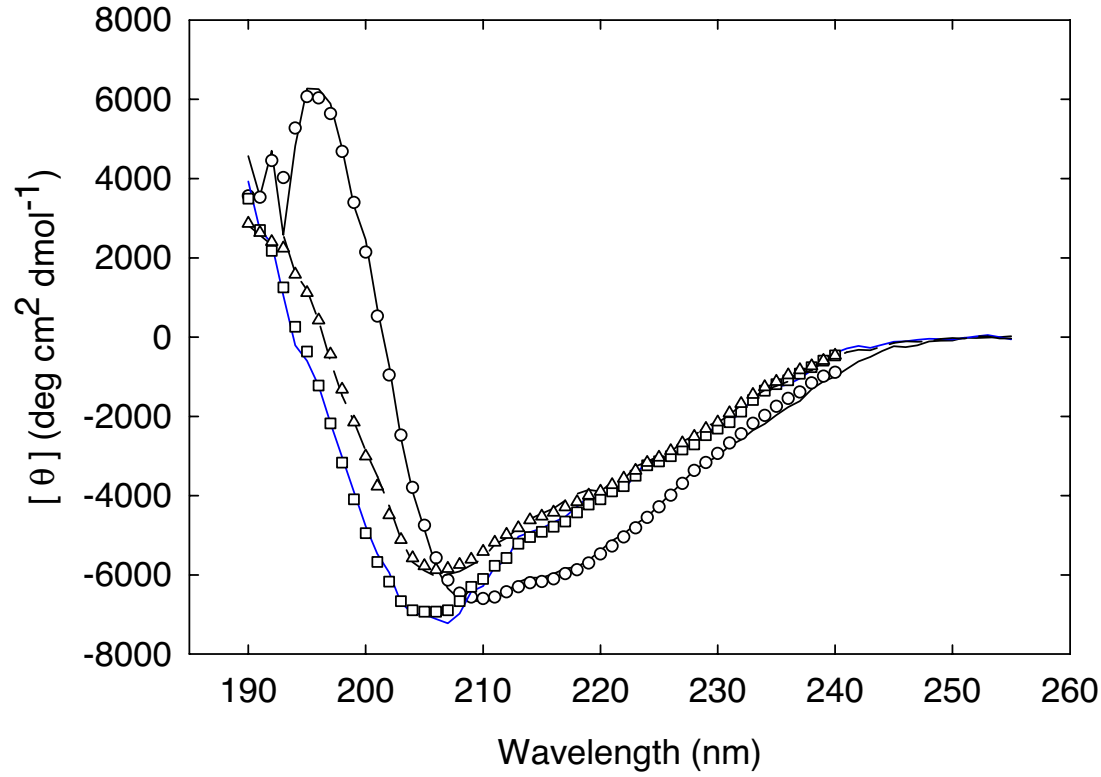

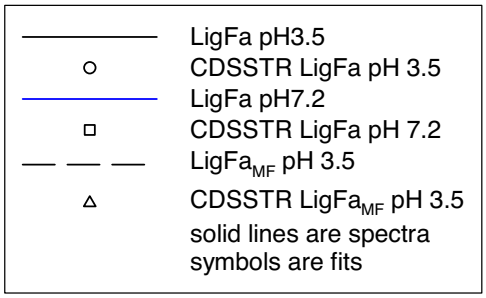

LigF&MF CDSSTRanalysis

	pH3.5	Δ(pH3.5->pH7.2)	Δ(native->MF)
helix	16	-10	-10
sheet	30	0	3
turn	21	-5	-5
unordered	32	15	12

Fig. S6. CD experimental data and model fit. Superimposition of the best fitting CD analysis method onto experimental CD data.

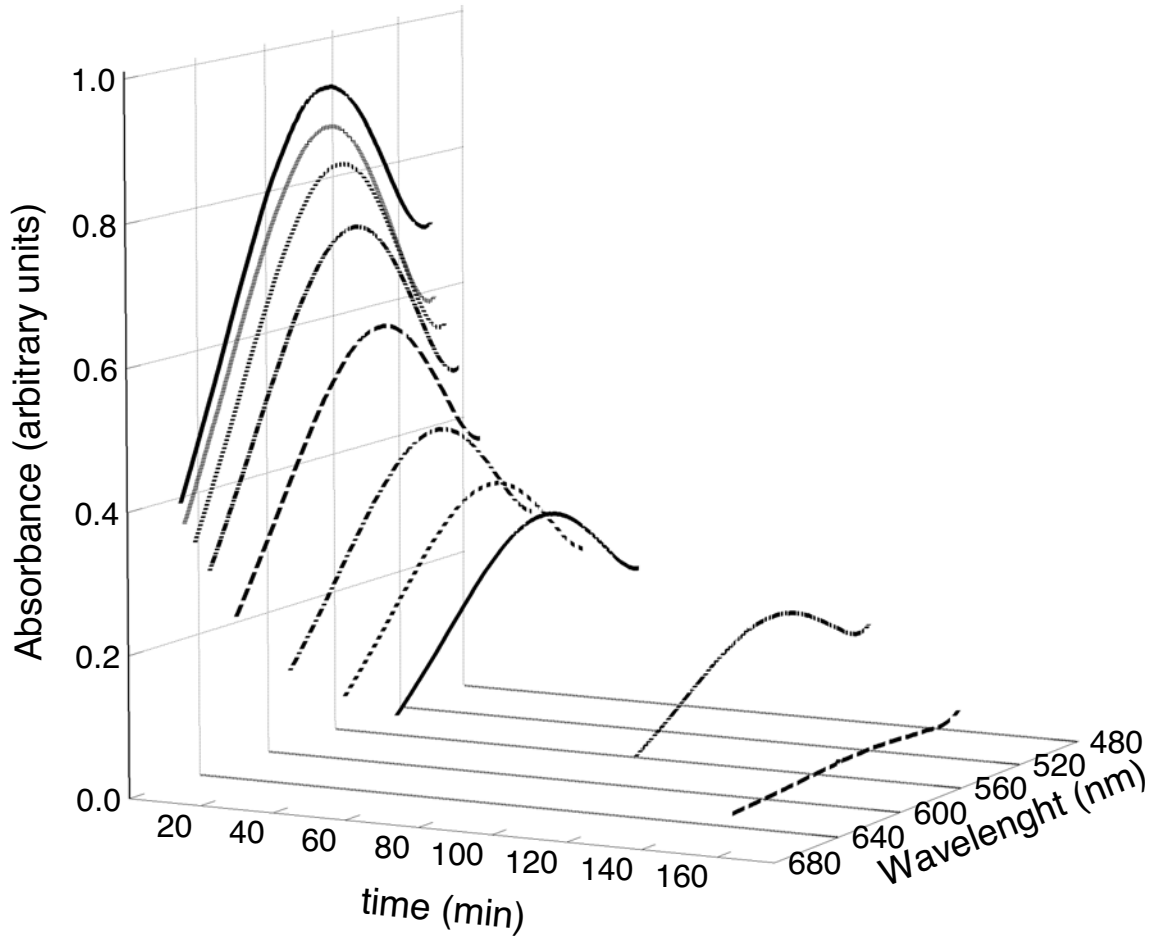

Fig. S7. Time-course of absorption spectra changes in response to dithionite treatment of LigFa protein. Reduction assays were done in 100 mM sodium citrate buffer, pH 3.5 and the UV-Vis spectra were recorded at different time intervals. The characteristic absorption has λ_{max} at 564 nm. [E] = 1.0 mM, [Dithionite] = 12.5 mM

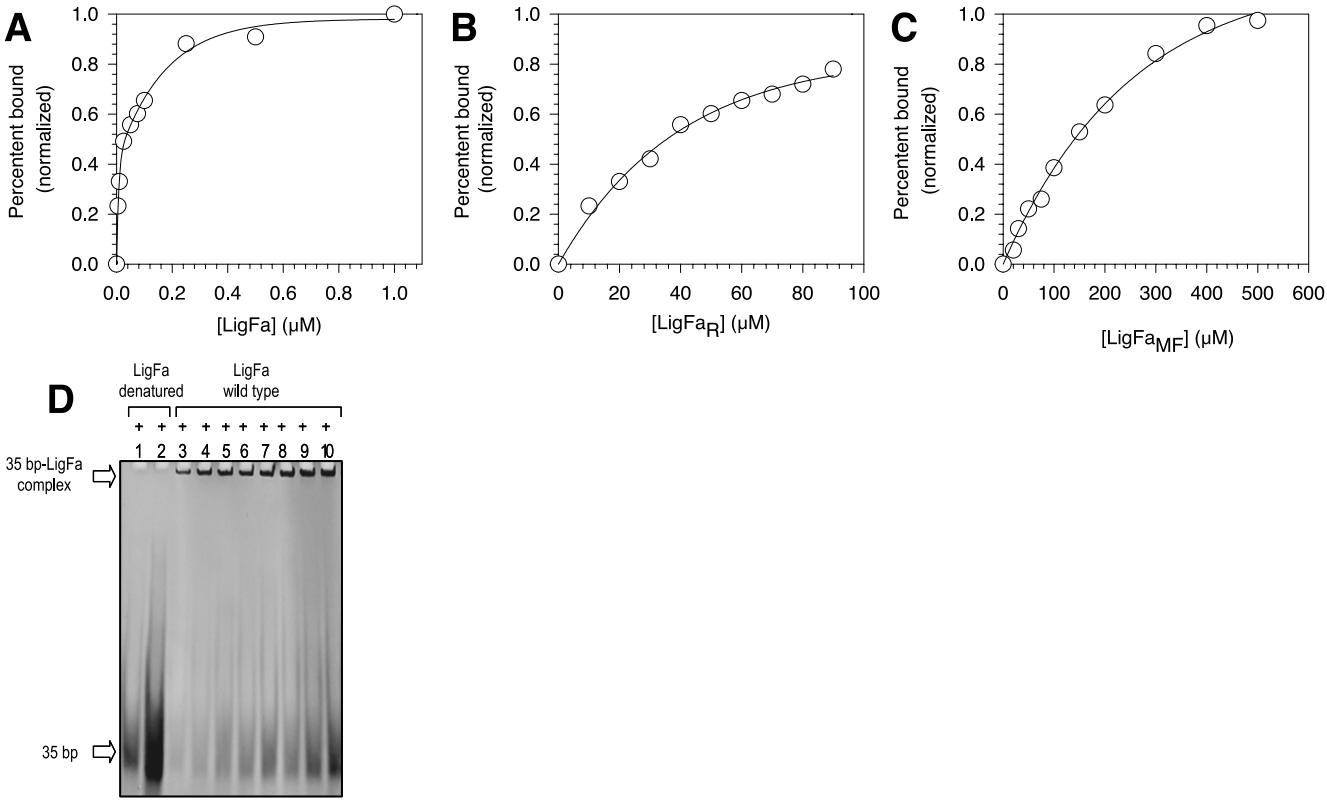

Fig. S8. Iron reduction and removal causes drastic reduction of DNA binding. DNA binding activities of LigFa forms differing in iron status: (*A*) LigFa, (*B*) LigFa$_R$, reduced iron form, and (*C*) LigFa$_{MF}$, metal-free form of the enzyme. Shown are the abilities of the different forms of LigFa to bind a radiolabelled, double-stranded ^{32}P-labeled 35 bp DNA substrate as measured by an EMSA assay. Note the scale differences on the X-axes (substrate concentration). (*D*) Polyacrilamide gel autoradiograph showing the differential interaction of LigFa with ^{32}P-labeled 35bp double strand oligonucleotide (EMSAs with LigFa were carried out as described in *SI Text*). The arrows indicate the double strand 35 bp sequence and the DNA-protein complex. *Lane 1*: denatured LigFa plus 1 μM ^{32}P-labeled 35 bp; *Lane 2*: denatured LigFa plus 10 μM ^{32}P-labeled 35 bp. As shown, no DNA-protein complex was formed when denatured protein was used, indicating that non-specific DNA binding occurs. *Lanes 3–10*: LigFa plus 0.02, 0.05, 0.075, 0.10, 0.15, 0.25, 0.50, 1.0 μM ^{32}P-labeled 35 bp. As shown in lanes 3–10 DNA binding occurs at very low DNA concentration when oxidized DNA LigFa was used. Measurement of LigFa-DNA complexes shown in A-C by the EMSA assay was done by densitometric scanning of polyacrilamide gels autoradiograph.

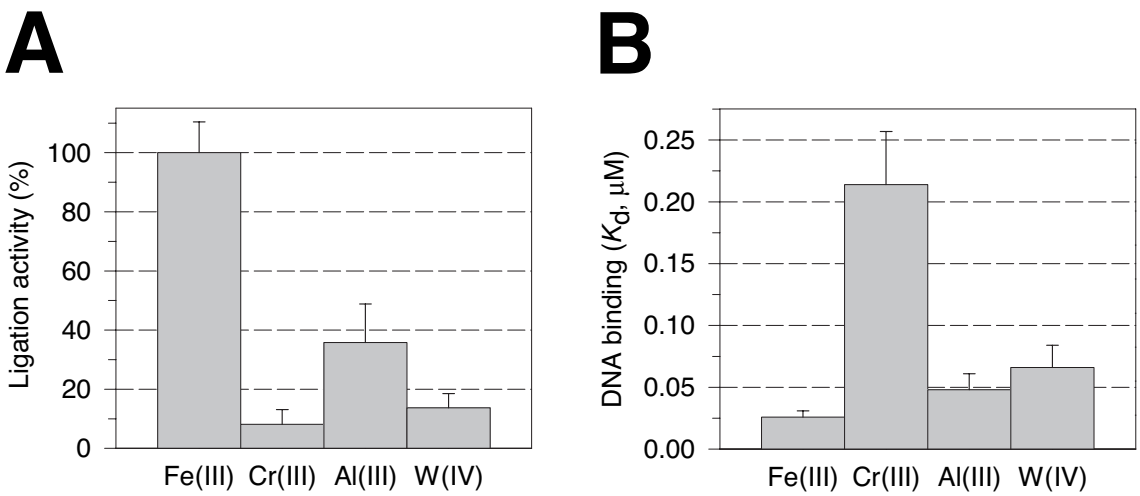

Fig. S9. Al^{3+}, W^{4+} and Cr^{3+} can poorly substitute Fe^{3+} in LigFa. (*A*) Ligation activity of metal LigFa variants (assay conditions as in Fig. 1). (*B*) DNA binding constant of metal LigFa variants. Protein–DNA complexes and the intensity of bands were approximately quantified by autoradiogram densitometry and by volume integration, respectively. Metal containing proteins were prepared as described in text. As shown, Cr^{3+}, Al^{3+} and W^{4+} produced LigFa variants that were able to bind DNA (*B*), although less efficiently than the ferric species. The binding constants were in the order $LigFa_{Cr}^{3+} \gg LigFa_{W}^{4+} > LigFa_{Al}^{3+} > LigFa_{Fe}^{3+}$: 214 ± 42.7, 66 ± 18, 48 ± 13 and 26 ± 5 nM, respectively. No other metal tested bound DNA. The same metal variants of LigFa also ligated substrate, although again with much lower activities than $LigFa_{Fe}^{3+}$ (Al 36%, W 17%, and Cr 4% of the iron-containing enzyme) (*A*).

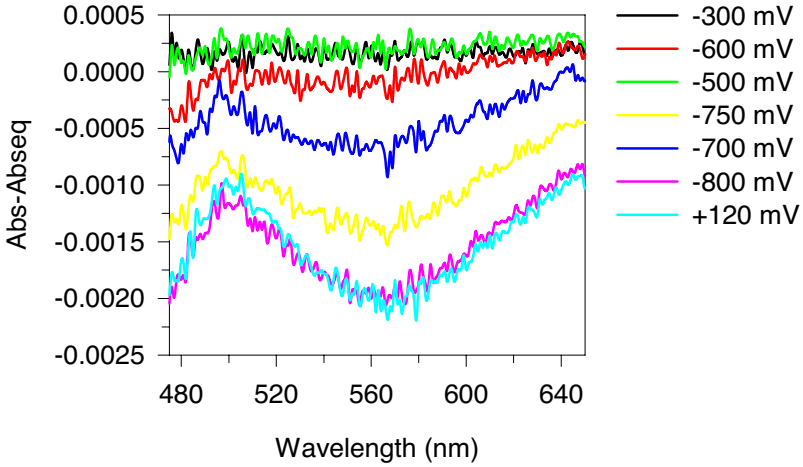

Fig. S10. Iron (III) in LigFa does not act as redox element. A typical collection of spectra for the reduction of LigFa-Fe^{3+} in the presence of methyl viologen (redox potential: -449 mV) at various applied potentials and 100 mM citrate buffer pH 3.5. [Methyl viologen] = 50 μM (from a stock solution of 0.5 mM in 2M KCl); [E] = 0.88 mM. Equilibrium redox potential of electrode itself: 121 mV. Path length: 8 μm. Here we investigated the possibility of a functional role of iron cations in LigFa as a redox elements by monitoring spectral changes associated with the reduction of LigFa at different applied potentials. Initially, at -300 mV, only the absorbance of LigFa associated with Fe^{3+} was observed and this signal was used as a background.

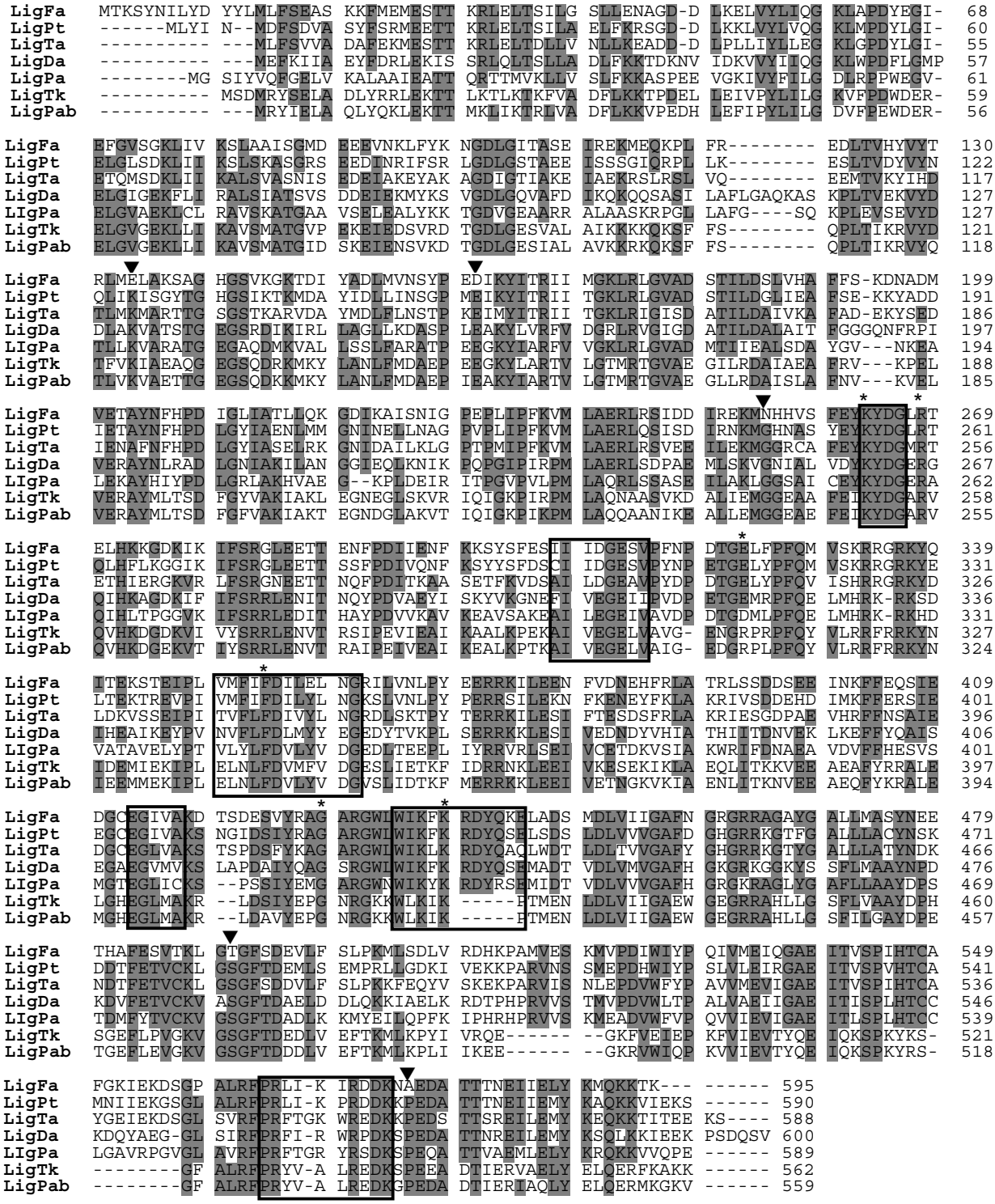

Fig. S11. Sequence alignment of archaeal DNA ligases. Source organisms and accession numbers are as follows: Fa, *Ferroplasma acidiphilum* (AJ850915); Pt, *Picrophilus torridus* (NC_005877.1); Ta, *Thermoplasma acidophilum* (AL445066.1); Da, *Desulfurolobus ambivalens* (Q02093); Pa, *Pyrobaculum aerophilum* (U82370); Tk, *Thermococcus kodakaraensis* (AB042527); Pab, *Pyrococcus abyssi* (B75173). Boxes represent the motifs commonly found in ATP-dependent DNA ligases. Arrow indicates those amino acids which were used to construct LigFa mutant variants with altered pH optimum.

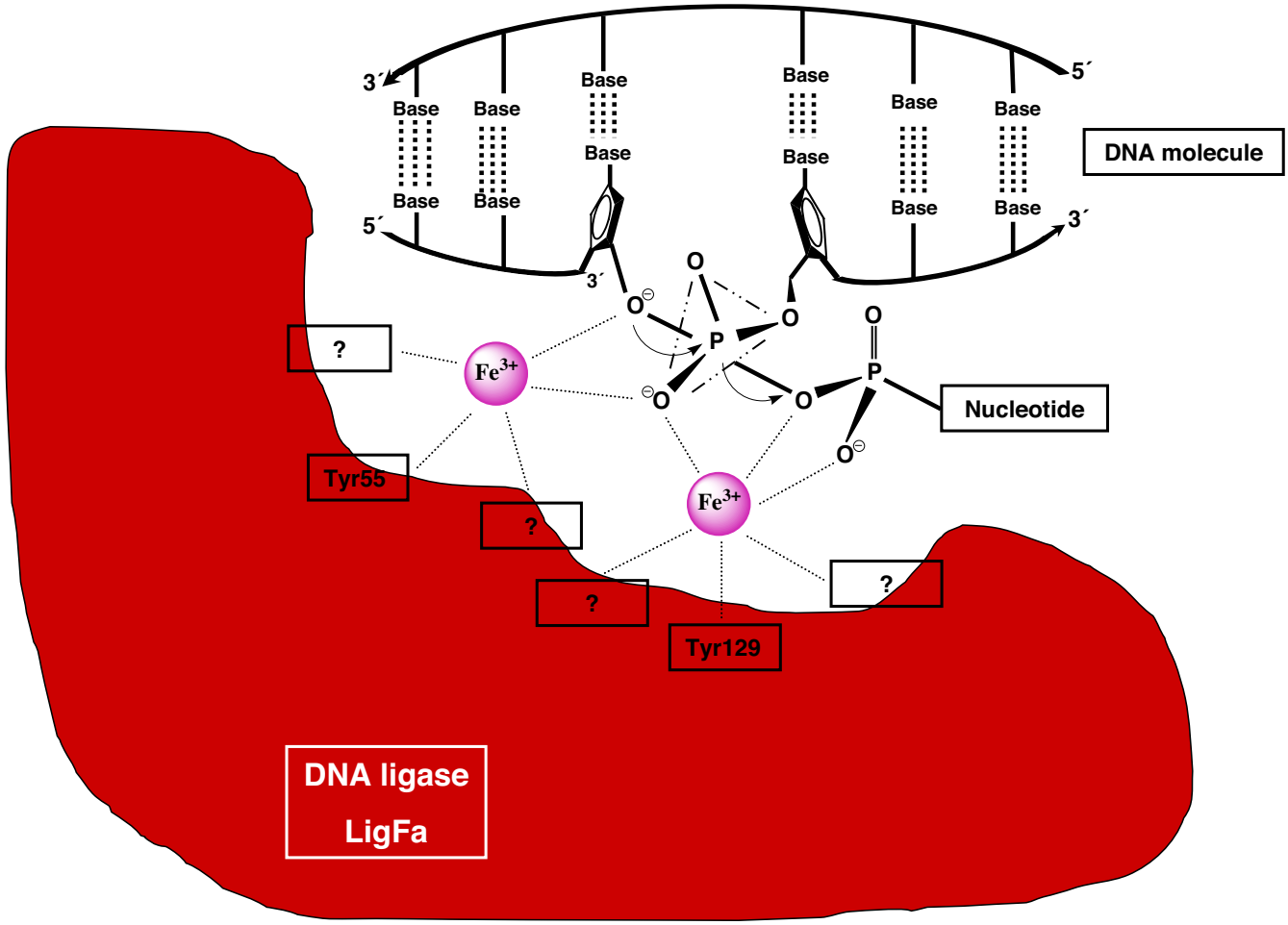

Fig. S12. Possible interactions of iron (III) clusters found in LigFa with DNA, nucleotide cofactor and DNA ligase. As shown the suggested possible interactions are similar to those associated to Mg(II) cations in ''common'' DNA ligases. The interactions of iron (III) irons with Tyr-55 and Tyr-129 are based on the results of site-directed mutagenesis experiments. Other possible iron (III) ligands in LigFa are shown with ''?'' symbol.

Table S1. Cofactor specificities of DNA ligases of acidophiles

	LigFa (40°C, pH 3.0)	LigFa (Phe^{192}→Ser^{192}) (40°C, pH 7.0)*	LigAf (40°C, pH 7.0)	LigTa (70°C, pH 6.5)	LigPt (70°C, pH 6.5)	LigSa (80°C, pH 7.5)
No cofactor	0.35 ± 0.04	–	0.06 ± 0.01	0.49 ± 0.06	0.02	0.12 ± 0.06
ATP	3.57 ± 0.57	0.41 ± 0.11	6.19 ± 0.60	4.94 ± 0.53	2.11 ± 0.27	12.39 ± 0.61
NAD^+	3.01 ± 0.47	–	0.06 ± 0.01	0.75 ± 0.07	0.75 ± 0.12	0.12 ± 0.07
dATP	0.35 ± 0.03	0.08 ± 0.03	0.16 ± 0.04	0.48 ± 0.06	0.25 ± 0.03	4.33 ± 0.45
AMPPNP	1.00 ± 0.21	–	0.25 ± 0.09	1.33 ± 0.15	0.08 ± 0.02	1.73 ± 0.11
GTP	0.36 ± 0.07	–	2.35 ± 0.35	0.48 ± 0.08	0.02	1.66 ± 0.10
CTP	0.30 ± 0.05	–	1.42 ± 0.23	0.48 ± 0.07	0.02	0.76 ± 0.08
UTP	0.35 ± 0.05	–	0.86 ± 0.10	0.46 ± 0.06	0.02	0.12 ± 0.06

The values shown are the k_{cat} kinetic constants (in min^{-1}) that were obtained in assays carried out by using a fluorimetric standard assay based on the ligation of a 5′-phosphorylated 35-mer to a 5′-fluorescein-labelled 25-mer annealed to the complementary 70-mer. Assays were carried out at the indicated optimal temperatures and pH values. pH was adjusted at 25°C. Nucleotide cofactors were provided at a concentration of 0.1 mM. All experiments were performed in triplicate (average value are shown, with standard deviation being lower than 5%). Values were obtained by Eadie–Hofstee linearization. – indicates that no ligation product was detected. As shown here, in the absence of nucleotide cofactor, LigFa was inactive: maximal activities were restored by addition of either ATP or NAD^+ (<zsi;st1>Table S1), which therefore appear to be cognate cofactors of the enzyme. Lower activities were obtained with the ATP analogue AMPPNP (30% of that with ATP), which can be hydrolyzed to AMP (but not to ADP), and dATP (10% activity). Other nucleoside triphosphates failed to substitute ATP. LigPt and LigTa had similar cofactor specificities, so these three enzymes are similar to previously reported cofactor requirements of DNA ligases of *Thermococcus kodakaraensis*, *Thermococcus fumicolans*, and *Pyrococcus abyssi* (1, 2). In contrast, LigSa and LigAf were ATP-dependent (in the case of LigSa, ATP could be substituted by dATP and, to a lesser extent, by GTP and AMP-PNP, and, in the case of LigAf, by GTP/CTP and to a lesser extent by UTP), but not NAD^+-dependent. *Reaction was done in phosphate buffer pH 7.0 in the presence of 0.5 mM $MgCl_2$. In the absence of metal cofactor no reaction was detected.

Table S2. Characterization of LigFa variants containing Tyr → Thr mutations

Variant	Iron content (mol Fe/mol protein)*	Activity† (k_{cat}: min^{-1})	Absorbance at 564 nm (arbitrary units)‡
LigFa	2.03 ± 0.09	3.57 ± 0.57	0.302
Tyr^{5}	2.01 ± 0.40	3.62 ± 0.53	0.329
Tyr^{9}	2.03 ± 0.40	3.65 ± 0.54	0.323
Tyr^{11}	2.00 ± 0.40	3.59 ± 0.52	0.327
Tyr^{12}	2.14 ± 0.43	3.82 ± 0.54	0.350
Tyr^{55}	0.07 ± 0.01	0.08 ± 0.01	0.057
Tyr^{65}	2.00 ± 0.39	0.62 ± 0.12	0.310
Tyr^{97}	1.97 ± 0.39	3.50 ± 0.33	0.323
Tyr^{127}	2.09 ± 0.40	3.87 ± 0.52	0.356
Tyr^{129}	0.02 ± 0.01	0.13 ± 0.04	0.023
Tyr^{151}	2.14 ± 0.42	3.71 ± 0.46	0.341
Tyr^{159}	2.15 ± 0.42	3.73 ± 0.44	0.349
Tyr^{165}	2.21 ± 0.44	3.41 ± 0.46	0.338
Tyr^{204}	2.24 ± 0.45	2.57 ± 0.49	0.341
Tyr^{262}	2.26 ± 0.45	3.58 ± 0.56	0.349
Tyr^{264}	2.17 ± 0.44	3.36 ± 0.48	0.331
Tyr^{303}	2.17 ± 0.43	3.55 ± 0.45	0.324
Tyr^{338}	2.20 ± 0.44	3.28 ± 0.43	0.312
Tyr^{369}	2.18 ± 0.43	3.33 ± 0.39	0.315
Tyr^{426}	2.23 ± 0.44	3.33 ± 0.38	0.313
Tyr^{442}	2.28 ± 0.46	3.34 ± 0.36	0.323
Tyr^{468}	2.33 ± 0.46	3.57 ± 0.46	0.334
Tyr^{528}	2.28 ± 0.46	3.66 ± 0.44	0.324
Tyr^{588}	2.27 ± 0.45	3.42 ± 0.32	0.326

*Results, calculated by HR-ICP-MS, are the average of data calculated from three independent samples ± SD.

†k_{cat} values were calculated as described in Table 1. Results are the average of data obtained from three independent samples ± SD.

‡All experiments were performed in triplicate (average value of λ_{max} at 564 nm are shown, with SD being lower than 8%).